AN ANALYTICAL APPROACH TO TRIMMING AND PERFORMANCE COUPLING ON FLYING WINGS

Matthieu Scherrer [1,2], Nicolas Quendez [1] , Carsten Döll[2,1,3]

[1] SUPAERO, 10 av Ed. Belin, B.P. 4032, F–31055 Toulouse Cedex, France

[2] ONERA–CERT, Systems Control and Flight Dynamics Department, 2, av Ed. Belin, B.P. 4025, F–31055 Toulouse Cedex, France

[3] Corresponding author : doll@cert.fr, Tel.: +33 (0)5.62.25.29.20, Fax : +33 (0)5.62.25.25.64

Keywords: *Flying Wing, Trimming Ability, Trim Drag, Cruise Performance, Take off Distance, Conceptual Design.*

Abstract

An original parameterization of the aerodynamic coupling between trimming and performance of a Flying Wing will be proposed. This will lead to an analytical model for trimming and performance coupling on flying wing, very useful at conceptual stage.

An analytical evaluation of the performance of the trimmed Flying Wing at conceptual stage will then be presented.

Assumptions and models

1 An innovative approach

1.1 Span loading : an inverse approach

It is usual to compute the lift distribution along span from wing planform and twist distribution. The effect of aspect ratio λ, sweep ϕ and taper ratio ε on span loading have been studied to a certain extent [1]. However those studies do not cover a wide range of geometries. Furthermore, the performance is not easy to parameterize.

An alternative approach will here be proposed, it is *an inverse approach* : The span loading will be considered as a conceptual input. The geometry that leads to this span loading will hence be obtained as an output.

This is a very powerful approach, and the process is quite a physical approach at the end. Providing the requested span loading is *realistic*, it is possible to find an accurate twist distribution that creates the targeted span loading for any planform.

Such a tool, using numerical optimization routines, has been implemented using Matlab. A lifting surface aerodynamics program called AILESPRIT computes the circulation distribution along span. Twist distribution is parameterized for implementing into optimization routines. After the optimization process has converged to the targeted span loading, the physical twist distribution solution to the problem is obtained for one flight condition. This approach offers the exact calculation of the cruising point.

The method can be extended to other flight conditions, under the assumption that a "rubber-like twist flying wing" is considered. The twist could be adjusted. This will give a very useful method for conceptual use, for modelling the complex aspect of trimming and performance coupling on flying wings.

Nota : Such an idealistic flying wing can be very fairly approached with an accurate set of flaps along trailing edge : this was done on a particular example.

1.2 Trimming ability

The work detailed in [2, 3] leads to the definition of a new conceptual variable : the *trimming ability*, particularly interesting for flying wing configurations.

This variable expresses the "performance in trimming" of a given planform, associated to a span loading and static margin. In few words, trimming ability quantifies the "pitch-up" or "pitch-down" effect of the lift distribution associated to the planform, at the neutral point location.

The balance of pitching moment on a trimmed Flying Wing aircraft, for a given static margin M_{Stat} and wing lift coefficient C_L, can be written as :

$$\begin{cases} Cm_{NP} - M_{Stat} C_L = 0 \\ Cm_{NP} = Cm_{Geom} + Cm_{Airf} \end{cases} \quad (1)$$

The total pitching moment at neutral point Cm_{NP} is split into Cm_{Geom}, the pitching moment created at neutral point by the local lift $l(y)$ applied at local quarter chord point and Cm_{Airf}, the pitching moment due to the airfoil over the whole wing.

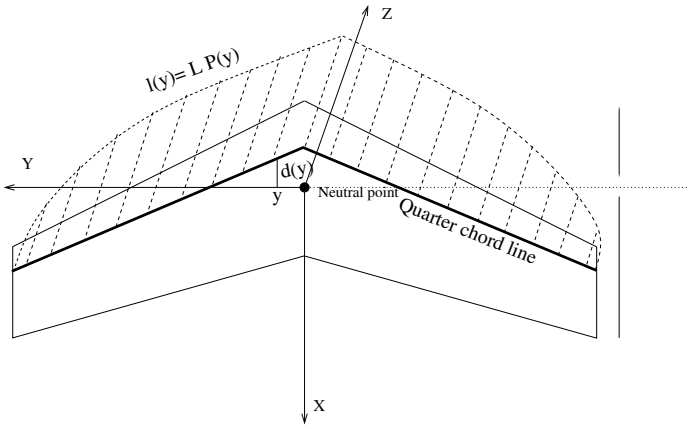

Fig. 1 Sketch for calculation of Cm_{Geom}, the pitching moment created by the local lift $l(y)$.

The local lift is defined by $l(y) = LP(y)$ where L is the total lift and $P(y)$ the span loading form. Cm_{Geom} is determined by the momentum equation :

$$Cm_{Geom} = \frac{2}{\rho S V^2 \mathrm{MAC}} \int l(y) d(y) dy$$

where d is the lever arm from quarter chord line to wing neutral point and MAC is the Mean Aerodynamic Chord. Then the trimming ability ξ can be defined as follows [3] :

$$\xi = \frac{Cm_{Geom}}{C_L} = \frac{1}{\mathrm{MAC}} \int P(y) d(y) dy \quad (2)$$

Trimming ability is hence a function of planform geometry $(\lambda, \varepsilon, \phi)$ through d and MAC, and of local lift distribution through the span loading form P : $\xi(d_{\lambda,\varepsilon,\phi}, P)$.

1.3 Span loading issue

Since span loading is considered as a conceptual variable, a proper span loading form is to be used. Proper span loading must be both realistic and useful to the overall performance. We shall also choose span loading in order to be able to handle it analytically.

1.3.1 Choosing two basic span loadings

Two different basic span loading were studied : minimum induced drag distribution l_{ell}, and so called "bell shaped" distribution l_{bell}. They were chosen for their particular characteristics (see Table 1).

1.3.2 Combination of the basic span loadings

The more general linear combination of these two lift distributions can then be considered. This combination is fully determined by the interpolation factor called t :

$$l(t) = t\, l_{ell} + (1-t)\, l_{bell}$$

Although idealized, this combination will cover a wide range of span loading for conceptual design.

If the variable θ is used for describing the span, through the usual expression : $y = \frac{b}{2} cos(\theta)$,

	Elliptic distribution	"Bell shaped" distribution
Analytical form	$l_{ell}(y) = L_{tot}\ \frac{2}{\pi}\sqrt{1-\left(\frac{y}{b/2}\right)^2}$ or $l_{ell}(\theta) = \frac{L_{tot}}{2} sin(\theta)$	$l_{bell}(y) = L_{tot}\ \frac{8}{3\pi}\left(1-\left(\frac{y}{b/2}\right)^2\right)^{\frac{3}{2}}$ or $l_{bell}(\theta) = \frac{3L_{tot}}{4} sin^3(\theta)$
Positive aspects	- Minimize induced drag : $e = 1$	- Higher value for trimming ability - Solution for reducing bending moment while minimizing induced drag impact
Drawbacks	- Small values for trimming ability	- Quite high induced drag : $e = 0.75$

Table 1 The two basic span loading : pro and cons

some calculations lead to [1] :

$$l(t,\theta) = 2\rho b V^2 \frac{C_L}{\pi\lambda}\left(sin(\theta) - \frac{1-t}{3} sin(3\theta)\right) \tag{3}$$

This parameterization allows to calculate the resulting Oswald factor e through classical Multhopp's calculation [4] :

$$e(t) = \frac{1}{1+\frac{(1-t)^2}{3}} \tag{4}$$

Similarly, trimming ability is a function of t :

$$\xi(t) = t\ \xi_{ell} + (1-t)\ \xi_{bell} \tag{5}$$

Where ξ_{ell} is the trimming ability for an elliptic span loading, and ξ_{bell} the trimming ability for a "bell shaped" span loading, both applied on a given wing planform.

Nota : There is no need for the interpolation factor t to be kept within $[0,\ 1]$: calculation is exact for any value of t. However values over $t \geq 1$ leads to pitch down, high drag situation, that are not interesting.

1.4 Application to the swept tapered wing

For the study case of single tapered swept wing, trimming ability ξ has been tabulated thanks to AILESPRIT lifting surface code. Results were identified as an analytical function $\xi_P(\lambda,\varepsilon,\phi)$ of the planform $(\lambda,\varepsilon,\phi)$, for given span loading form P.

[1] For $t = 1$, elliptic span loading can easily be checked, as well as "bell shaped" for $t = 0$.

Tapered, swept wings have been treated over a wide range of plan-form (Sweep $\phi \in [-10,\ +60^o]$, taper ratio $\varepsilon \in [0.1,\ 1]$, aspect ratio $\lambda \in [4,\ 16]$). To reach a high level of accuracy over this whole range, it was necessary to consider the following polynomial function :

$$\begin{aligned}\xi_P(\lambda,\varepsilon,\phi) = {} & k_1 + k_2\phi + k_3\phi^2 + k_4\phi^3 \\ & + k_5\varepsilon\phi + k_6\varepsilon^2\phi + k_7\varepsilon\phi^2 + k_8\varepsilon\phi^3 \\ & + k_9\varepsilon\phi\lambda + k_{10}\varepsilon\phi^2\lambda \\ & + k_{11}\varepsilon\phi^3\lambda + k_{12}\varepsilon\lambda + k_{13}\phi\lambda + k_{14}\phi^2\lambda \\ & + k_{15}\phi^2\varepsilon^2\lambda + k_{16}\phi^3\varepsilon^2\lambda + k_{17}\lambda^2\end{aligned} \tag{6}$$

Values for "k" coefficient are given in appendix A. This function will be very useful in the evaluation of the performance under trimming constraint.

2 Dedicated models for drag and maximum lift of an airfoil on a finite wing

Due to the trimming issue, it is interesting for Flying Wing to consider the performance of an airfoil as a function of its pitching moment coefficient Cm_0.
Straightforward models will be presented in this paper, but could be replaced by more accurate ones.

2.1 Models for airfoil drag

Based on [5, 6], it can be illustrated that for a fixed Reynolds number, airfoil drag coefficient Cd_0 can be kept constant over the range of

pitching moment among classical airfoils ($Cm_0 \in [-0.1, 0.05]$).

To a certain extent, Cd_0 can be set independently from airfoil pitching moment, within this Cm_0 range, as a "technological value" (see Fig. 2).

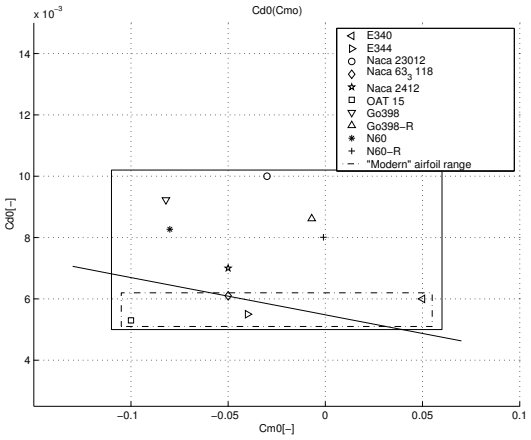

Fig. 2 Cd_0 as a function of Cm_0 among classical airfoils : a technological level.

A model for additional drag $\Delta Cd_0(\Delta Cm_0)$, caused by a flap deflection, is also derived from [5] (for more details see [2]) :

$$\Delta Cd_0 = 0.2487\,\Delta Cm_0{}^2 - 0.2509\,\Delta Cm_0{}^3 + 6.825\,\Delta Cm_0{}^4 \quad (7)$$

2.2 Models for airfoil maximum lift

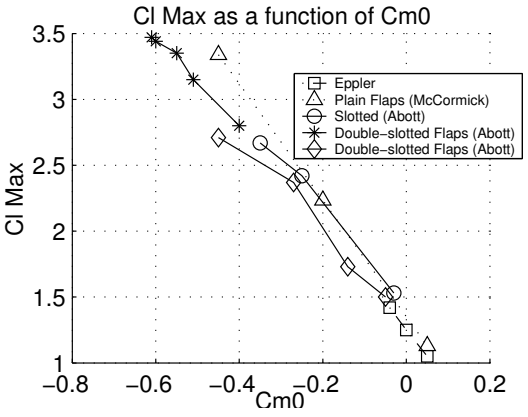

Fig. 3 Cl_{max} as a function of Cm_0.

According to data from [6, 7], maximum lift of the airfoil Cl_{max} can be considered as a linear function of pitching moment Cm_0, including high lift device cases as depicted in Fig. 3 : the more negative Cm_0, the higher Cl_{max}.

2.3 Conversion from bidimensional to tridimensional data

For use on a finite wing, some relationships have to convert the airfoils wind tunnel data to more accurate "airfoil on a finite wing" data.

2.3.1 *Pitching moment $Cm_{Airfoil\ 3D}$ of the wing*

The effective pitching moment of an airfoil *over a finite wing* called, $Cm_{Airfoil\ 3D}$, taken at the wing neutral point, is not exactly the airfoil's Cm_0. This was studied thanks to AILESPRIT and expressed as followed :

$$Cm_{Airfoil\ 3D}(\varepsilon,\phi,Cm_0) = Cm_{3D0}(\lambda,\varepsilon,\phi) + \Psi(\varepsilon,\phi)\,Cm_0 \quad (8)$$

Functions Cm_{3D0} and Ψ are detailed in appendix B.

2.3.2 *Maximum lift C_{Lmax} of the wing*

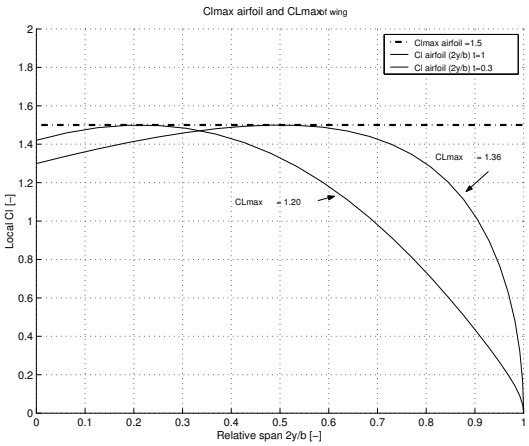

Fig. 4 The relationship between airfoil Cl_{max} and wing C_{Lmax} depends on span loading "t".

The following definition for operational maximum lift C_{Lmax} of the wing is taken from [5] :

"Operational C_{Lmax} is reached as soon as anywhere along the wing span, local Cl_{max} is reached".

This is illustrated in Fig. 4. Local Cl_{max} is plotted along span when the operational maximum lift is reached, for two different value of "t". With a local $Cl_{max} = 1.5$, the reached wing C_{Lmax} is 1.36 for $t = 1$, for $t = 0.3$, just $C_{Lmax} = 1.2$ can be reached.

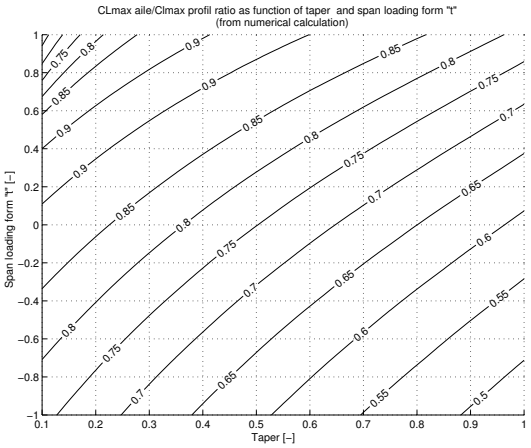

Fig. 5 The relationship between wing C_{Lmax} and airfoil Cl_{max} as function of taper ε and "t".

It can furthermore be shown that the relationship between Cl_{max} and C_{Lmax} just depends on taper ratio ε and span loading form parameter "t", as seen on Fig. 5. Thanks to the inverse approach, it is not a function of λ and ϕ anymore.

3 Model for CD_i constrained by trimming

From the innovative approach explained before, an analytical model for induced drag coefficient CD_i, constrained by longitudinal trimming, can be derived.

The induced drag is expressed by Eq. 4. The trimming ability concept (1) in combination with Eq. (8) allows to quantify the effect of the span loading on the longitudinal balance :

$$\begin{cases} \text{Trimming constraint (1):} \\ \xi(\lambda,\varepsilon,\phi,t) = M_{Stat} - \frac{Cm_{Airfoil\ 3D}(\lambda,\varepsilon,\phi,Cm_0)}{C_L} \\ \text{Induced drag (2):} \\ CD_i(\lambda,t,C_L) = \frac{1}{\pi\lambda e(t)} C_L^2 \end{cases} \tag{9}$$

Reversing the trimming constraint leads to the choice of an accurate span loading (via the special value $t(Cm_0)$) that satisfies the longitudinal balance.

Then the level of induced drag due to this particular span loading is now known via the Oswald factor $e(t(Cm_0))$:

$$\begin{cases} t(Cm_0) = \frac{M_{Stat} - \frac{Cm_{3D0}(\lambda,\varepsilon,\phi)+\Psi(\varepsilon,\phi)Cm_0}{C_L} - \xi_{bell}(\lambda,\varepsilon,\phi)}{\xi_{ell}(\lambda,\varepsilon,\phi) - \xi_{bell}(\lambda,\varepsilon,\phi)} \\ e\left[t(Cm_0)\right] = \frac{1}{1+\frac{\left[1-t(Cm_0)\right]^2}{3}} \end{cases}$$

As a final result, the value of induced drag CD_i is obtained, that is a function of the whole set of the following variables :

- CD_i is a classical function of aspect ratio λ and lift coefficient C_L
- CD_i is also a function of the Oswald factor e. This factor is a function of planform geometry λ,ε,ϕ, lift coefficient C_L and static margin M_{Stat}, as a consequence of the span loading constrained by longitudinal balance via the value of $t(Cm_0)$.

It can be written formally by :

$$CD_i(\lambda,Cm_0,C_L)_{(\varepsilon,\phi,M_{Stat})} = \frac{1}{\pi\lambda e\left(t(Cm_0)_{(\lambda,\varepsilon,\phi,M_{Stat},C_L)}\right)} C_L^2 \tag{10}$$

This is the main result of this paper. This analytical result can be added to any other pre-design aerodynamic module within an optimization loop in order to take into account the trim condition on induced drag, *i.e.* the main part of trim drag.

Optimization of the trimmed Flying Wing conceptual performance

The models detailed before and the trimming ability concept will be combined in order to analyse analytically conceptual performance of a trimmed flying wing.

4 Minimizing drag in cruise flight : the concept of optimal airfoil

4.1 Optimal trimming in cruise flight

Our goal is here to minimize the trim drag for the cruising flying wing. Wing planform $(\lambda, \varepsilon, \phi)$, the static margin M_{Stat} and lift coefficient C_L are fixed.

No deflection drag ΔCd_0 is caused if flaps are not used for trimming in cruise. That means an accurate airfoil has to be chosen to trim the aircraft. According to §2.1, Cd_0 can be considered as constant.

On the other hand, induced drag Cd_i is expressed as a function of airfoil pitching moment in Eq. (10).

As a result, only Cd_i is a function of Cm_0 within classical airfoil range (Fig. 6).

Then induced drag Cd_i can be minimized by searching the accurate value of airfoil pitching moment. Minimizing Cd_i corresponds to setting the maximum value for Oswald factor, that is $e = 1$[2].

Let us call $Cm_{0design}$ the value of airfoil pitching moment that allows to minimize induced drag Cd_i at $e = 1$, while respecting the trimming constraint Eq. 9-(1).

For given planform $(\lambda, \varepsilon, \phi)$, static margin M_{Stat} and lift coefficient C_L, choosing for the airfoil pitching moment the value $Cm_{0design}$ will ensure the designer that the trim drag is minimum. An "optimal cruising airfoil" with respect to the trimming constraint is defined.

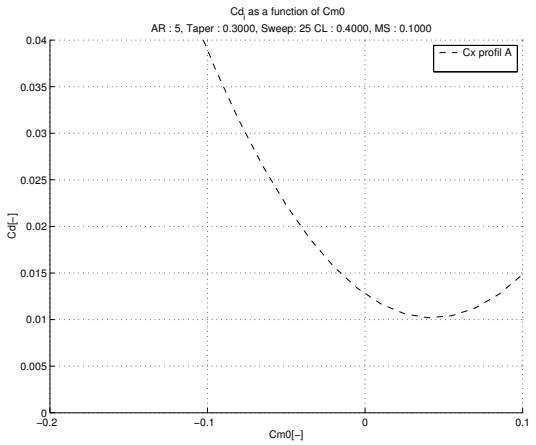

Fig. 6 Cd_i as a function of Cm_0 : a result from trimming.

This leads to the following value for the optimal pitching moment

$$\begin{cases} (Cm_{0design})_{approx} = [M_{Stat} - \xi_{elli}(\lambda, \varepsilon, \phi)]\, Cz \\ Cm_{0design} = \frac{(Cm_{0design})_{approx} - Cm_{3D0}(\lambda, \varepsilon, \phi)}{\Psi(\phi, \varepsilon)} \end{cases} \tag{11}$$

Nota : Up to now, transonic effects on lift have not been considered as there was no need to do so. The design parameter t is independent of transonic effects. Then the inverse problem must be solved. Transonic effects will interfere at this stage of the design, in particular during the determination of the actual twist. At the moment, our current tools solve the inverse problem just at low speed.

4.2 Parametric study for the "optimal airfoil"

4.2.1 Parametric effect of different variable

The "optimal cruising airfoil" with respect to the trimming constraint has been defined in §4.1, for a given planform $(\lambda, \varepsilon, \phi)$, given static margin M_{Stat} and lift coefficient C_L. This airfoil is characterized by its pitching moment, called $Cm_{0design}$.

The parametric effect of all parameters

[2]This is equivalent to set the lift distribution as elliptic in the inverse formulation of the problem.

$\lambda, \varepsilon, \phi, M_{Stat}$ and C_L on the optimal airfoil pitching moment $Cm_{0_{design}}$ has also been studied.

Let us now focus on the taper ratio ε effects on performance. Concerning aspect ratio, it is found that the higher the λ is, the more negative becomes the $Cm_{0_{design}}$.

4.2.2 *Parametric effect of taper ratio ε and sweep ϕ*

Taper effect on trimming has rarely been studied. However, taper appears to become a sizing parameter in the flying wing case, via the trimming constraint. Our approach allows to quantify this effect.

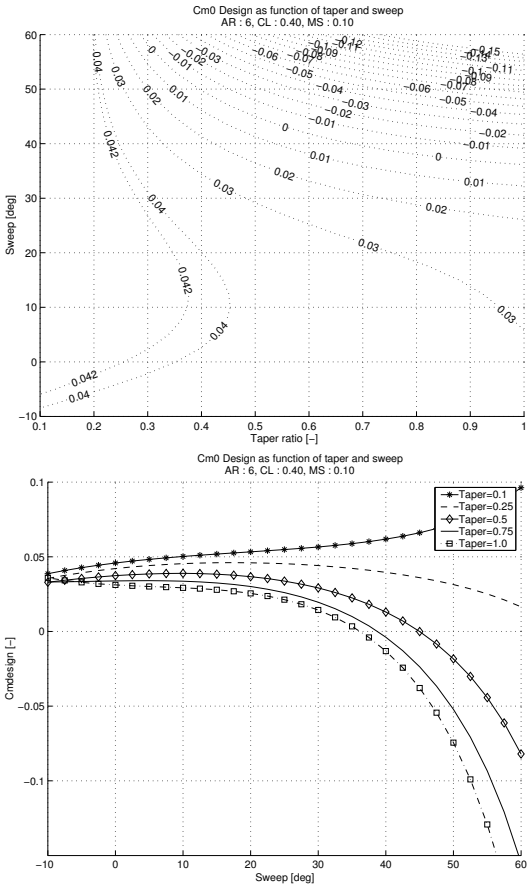

Fig. 7 $Cm_{0_{design}}$ as function of taper ratio ε and sweep ϕ.

On Fig. 7, the values for $Cm_{0_{design}}$ are plotted for given cruise C_L, static margin M_{Stat} and aspect ratio λ, as a function of taper ratio ε and sweep ϕ.

As expected, it can be noticed that generally speaking, the higher the sweep angle ϕ, the more negative $Cm_{0_{design}}$ gets. The sweep angle helps trimming.

But the effect of taper ε is unexpectedly important. If taper becomes close to $\varepsilon = 1$ (that is "square" wing), the more negative the $Cm_{0_{design}}$ is. On the contrary, if taper gets close to $\varepsilon = 0$, the effect of the sweep can be reversed !

Consequently, if you want to use a transonic airfoil ($Cm_0 \simeq -0.1$) that would be the optimal airfoil $Cm_0 = Cm_{0_{design}}$, you must choose high sweep and taper close to 1. On this example, this is not realistic (sweep up to 60 !). You might also release the constraint on aspect ratio λ (higher values) and the static margin M_{Stat}.

5 Minimizing conceptual take off distance under trimming constraint

5.1 Simple model for take off distance

The take off will just be considered from a performance point of view. The rotation phase is not taken into account. Conceptual take off distance TOD is hence the sum of ground distance, TOD_g, and the initial climb distance TOD_{climb} :

$$\begin{aligned} TOD &= TOD_g(C_{Lmax}) \\ &\quad + TOD_{climb}(C_{Lmax}, L/D) \end{aligned} \quad (12)$$

Ground distance TOD_g is linked to C_{Lmax}, whereas the initial climb distance TOD_{climb} is influenced by C_{Lmax} and L/D ratio.

The pitching moment Cm_0 reflects the high lift level : the more negative the pitching moment Cm_0 is, the higher the maximum lift C_{Lmax} will be allowed. Cm_0 is from now on not the result of an optimization process as it was in §4, but a parameter input standing for the setting of high lift devices which will be set within the interval $Cm_0 \in [-0.4, +0.1]$ for the following analysis .

The additional deflection drag, written as $\Delta Cd_0(Cm_0)$ can be computed using Eq. (7).

5.1.1 *Ground distance TOD_g*

During the ground run, the airspeed increases up to $V_{TakeOff}$, the speed corresponding to the oper-

ational maximum lift C_{Lmax}. The simple model from [8] is used, that gives TOD_g proportional to the following expression $\widetilde{TOD}_g$:

$$\begin{aligned} TOD_g(Cm_0) &\propto \widetilde{TOD}_g(Cm_0) \\ \widetilde{TOD}_g(Cm_0) &= \frac{(mg)^2}{S\, C_{Lmax}(Cm_0)\, F_{0.7}} \end{aligned} \quad (13)$$

where $F_{0.7}$ is the thrust when the speed is $0.7 V_{Take\,Off}$.

5.1.2 *Initial climb distance TOD_{climb}*

The initial climb is ruled by the thrust-to-weight ratio $\frac{F}{mg}$ and the effective L/D at the take off speed. According to [8], TOD_{climb} is the distance where the height h_{secu} is reached, projected to the ground :

$$TOD_{climb}(Cm_0) = \frac{h_{secu}}{0.81\frac{F_0}{mg} - L/D_{Take\,Off}(Cm_0)} \quad (14)$$

where F_0 is the thrust at $V = 0 m/s$ and $L/D_{Take\,Off}$ is a function of Cm_0 since it is defined as follows :

$$L/D_{Take\,Off} = \frac{C_{Lmax}(Cm_0)}{C_D(Cm_0)}$$

5.2 Maximum high lift level

Thanks to our approach, take off calculations are naturally done under trimming constraint.

Results are plotted on Fig. 8 : the greater the high lift level (*i.e.* the more negative the Cm_0), the shorter TOD_g, but also the longer the TOD_{climb}. TOD_{climb} is indeed strongly penalized by the additional trim drag through $L/D_{Take\,Off}$ from Eq. (14).

An optimal Cm_0 for minimum TOD appears. This Cm_0 is associated to a maximum allowable high lift level.

This work has been done for a Flying Wing configuration and a classical configuration (with a proper trim drag model). The comparison shows that the high lift maximum limit occurs much earlier for Flying Wing than for classical configuration, because of extra trim drag.

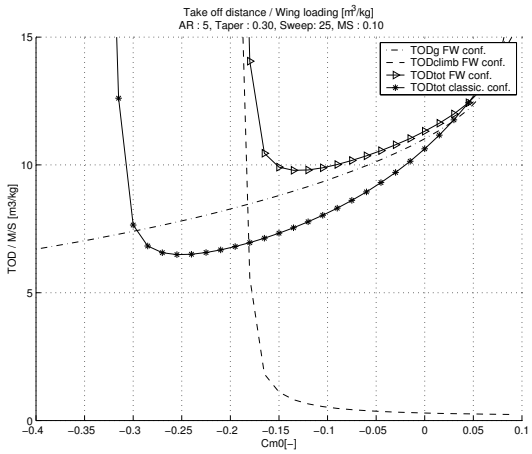

Fig. 8 Conceptual TOD detail. Comparison with classical configuration.

As a result, the minimum conceptual $\frac{TOD}{Wing\,Loading}$ is much longer for Flying Wing than for classical configuration. The following well known result is confirmed : lighter wing loading is needed on Flying Wing for the same TOD as classical configuration.

5.3 Parametric study of taper ratio ε

As for optimal airfoil, parametric sensitivity of each variable has been studied. Once again, we will focus on taper ratio ε.
Two effects are encountered :

1. On the one hand, taper close to $\varepsilon = 0$ causes higher trim drag (as for §4.2.2).

2. On the other hand, taper close to $\varepsilon = 0$ also allows higher values for wing C_{Lmax} for a given airfoil Cl_{max}, as shown on Fig. 5.

The predominant effect remains however the second effect, see Fig. 9 : taper close to $\varepsilon = 0$ reduces TOD due to the complex coupling between trimming and performance. It can be concluded that for the Flying Wing, taper can be tailored in order to improve take off performance with interesting results.

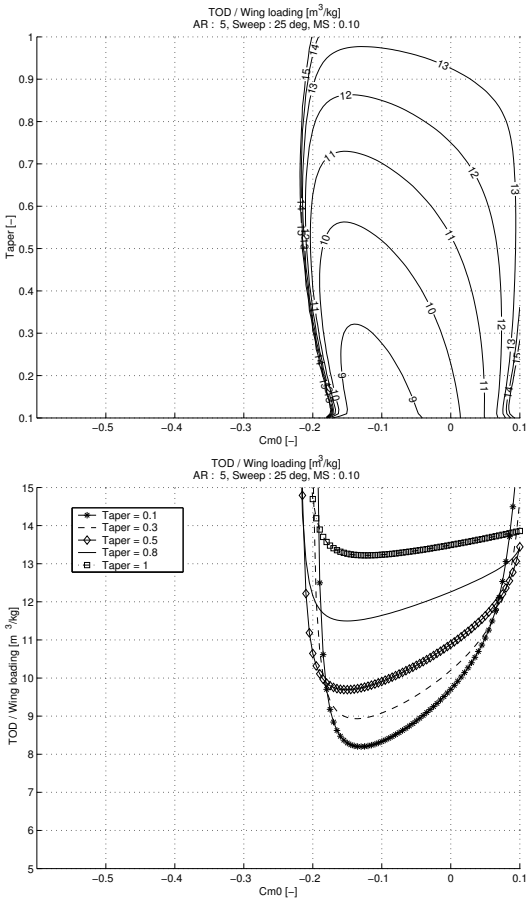

Fig. 9 Conceptual TOD as a function of taper ε and "high lift level" Cm_0.

6 Conclusions

An innovative approach was detailed for Flying Wing conceptual performance evaluation, proposing an inverse problem on span loading. The result is an analytical approach for the trimming and performance coupling.

Particularly, an independent expression for induced drag CD_i under trimming constraint was presented.

This approach was then illustrated on a conceptual optimization example.

For cruising flight, it was shown that an optimal airfoil, defined through its pitching moment $Cm_{0_{design}}$, can be properly chosen to minimize trim drag.

For take off, the performance gap compared with classical aircraft configuration was illustrated leading to some design rules.

References

[1] V.I. Stevens. Theoretical basic span loading characteristics of wings with arbitrary sweep, aspect ratio, and taper ratio. Technical Report Naca TN 1772, NACA, Naca, USA, December 1948.

[2] N. Quendez. Le code surface portante AilEsprit. Technical Note DCSD-T 145/2002, ONERA - UTC, 2, av Edouard Belin, BP 4025, F-31055 TOULOUSE, France, July 2002.

[3] N. Quendez. Optimisation de l'aérodynamique d'une aile volante. Master Thesis DCSD-T 144/2002, ONERA - UTC, 2, av Edouard Belin, BP 4025, F-31055 TOULOUSE, France, July 2002.

[4] H. Multhopp. The calculation of lift distribution of wings. *Luftf. Forschung*, 15:153ff, 1938.

[5] B.W. McCormick. *Aerodynamics, Aeronautics and Flight Mechanics*. Wiley and Sons, 2nd edition, August 1994.

[6] I.H. Abbott and A.E. Von Doenhoff. *Theory of Wing Section & A Summary of Airfoil Data*. Dover Publication, 2nd edition, 1959.

[7] R. Eppler. *Airfoil design and data*. Springer Verlag, 1990.

[8] J.L. Boiffier. *The dynamics of flight : The equations*. John Wiley & Sons, Hoboken, Chichester, Weinheim, Singapore, Mitton, 1st edition, August 1998. Chp. 10 : Take–Off and Landing.

[9] M. Scherrer. Modélisation & optimisation du couplage aérodynamique Équilibrage - performance sur les ailes volantes. Technical Report DCSD-T 178/2003, ONERA-SUPAERO, 2, av Edouard Belin, BP 4025, F-31055 TOULOUSE, France, August 2003.

A Trimming ability for the swept tapered wing

The values k_i of Eq. (6) for elliptical span loading are :

$$\begin{array}{lcrlcr}
k_1 &=& 2.0624\,10^{-3} & k_2 &=& 2.8635\,10^{-4} \\
k_3 &=& 7.2193\,10^{-5} & k_4 &=& -5.1723\,10^{-7} \\
k_5 &=& -6.3268\,10^{-3} & k_6 &=& 1.7347\,10^{-3} \\
k_7 &=& -1.3713\,10^{-5} & k_8 &=& 2.4930\,10^{-7} \\
k_9 &=& 1.0896\,10^{-3} & k_{10} &=& 1.9649\,10^{-5} \\
k_{11} &=& 1.3099\,10^{-7} & k_{12} &=& 5.8523\,10^{-5} \\
k_{13} &=& -2.5644\,10^{-4} & k_{14} &=& -5.5720\,10^{-6} \\
k_{15} &=& -2.7188\,10^{-5} & k_{16} &=& 2.0751\,10^{-7} \\
k_{17} &=& -6.0909\,10^{-5} & & &
\end{array}$$

The values k_i of Eq. (6) for "bell shaped" span loading are :

$$\begin{array}{lcrlcr}
k'_1 &=& -2.7271\,10^{-3} & k'_2 &=& 3.6980\,10^{-3} \\
k'_3 &=& -8.0429\,10^{-5} & k'_4 &=& 1.2723\,10^{-6} \\
k'_5 &=& -5.6574\,10^{-3} & k'_6 &=& 5.2503\,10^{-4} \\
k'_7 &=& -2.1094\,10^{-5} & k'_8 &=& 3.3288\,10^{-7} \\
k'_9 &=& 1.4932\,10^{-3} & k'_{10} &=& 4.7188\,10^{-6} \\
k'_{11} &=& 4.3625\,10^{-7} & k'_{12} &=& -8.7402\,10^{-4} \\
k'_{13} &=& 1.3622\,10^{-4} & k'_{14} &=& 4.1099\,10^{-6} \\
k'_{15} &=& -2.4646\,10^{-5} & k'_{16} &=& 8.3283\,10^{-8} \\
k'_{17} &=& -1.1869\,10^{-5} & & &
\end{array}$$

B Wing pitching moment $Cm_{Airfoil\ 3D}$

The wing pitching moment $Cm_{Airfoil\ 3D}$ is given by Eq. (8) as :

$$Cm_{Airfoil\ 3D}(\varepsilon,\phi,Cm_0) = Cm_{3D0}(\lambda,\varepsilon,\phi) + \Psi(\varepsilon,\phi)\,Cm_0$$

with :

$$\begin{aligned}
Cm_{3D0}(\lambda,\varepsilon,\phi) &= k_a + k_b\phi^2 + k_c\lambda + k_d\varepsilon \\
\Psi(\varepsilon,\phi) &= k_\alpha + k_\beta\phi + k_\gamma\phi^2 + k_\delta\varepsilon\phi \\
&\quad + k_\sigma\varepsilon + k_\zeta\varepsilon^2
\end{aligned}$$

where :

$$\begin{cases}
k_a = 2.27544040364\,10^{-3} \\
k_b = -1.89047090\,10^{-6} \\
k_c = -3.6058065218\,10^{-4} \\
k_d = 9.33053537282\,10^{-3}
\end{cases}$$

$$\begin{cases}
k_\alpha = 8.1905745765293\,10^{-1} \\
k_\beta = 5.377947288\,10^{-4} \\
k_\gamma = -1.2433649855\,10^{-4} \\
k_\delta = -1.34709072940\,10^{-3} \\
k_\sigma = 3.3437468167639\,10^{-1} \\
k_\zeta = -1.75721993498\,54\,10^{-1}
\end{cases}$$